An Integrated Model for Urban Microclimate and Building Energy in High-Density Cities for Early Stage Design

Jianxiang Huang[1], Phil Jones[2], Rong Peng[1], Xiaojun Li[2], Shanshan Hou[2]

[1]Department of Urban Planning and Design, Faculty of Architecture, the University of Hong Kong, Hong Kong SAR China

[2]Architectural Science Group, Welsh School of Architecture, Cardiff University, UK

Abstract

The energy performance of an urban building depends on its surroundings. Existing building energy models are limited in accounting for micro-scale variations of the surrounding environment, which may significantly modify building energy performance in high-density cities. Modeling of building energy at urban scale remains a nascent field. This paper presents an integrated urban microclimate (UMM) and building energy model (HTB2), which has been developed to assess the energy performance of a cluster of buildings and their external environments in high-density cities. The simulation results were evaluated by comparison with field measurement data collected from the Sai Ying Pun neighbourhood in Hong Kong. The model has potentials to support building design and urban planning at early stage.

Introduction

A building and urban microclimate are highly interconnected in cities. From a thermal perspective, the building modifies its surrounding microclimate, affecting sunlight, wind, and temperature. This modification in turn affects its own energy performance and those buildings nearby. Overshadowing by neighbouring buildings affects solar radiation incident on the buildings facades; temperature fluctuation of external wall surfaces modifies long-wave heat exchanges; wind shadowing affects external heat flux. Air temperature in street canyons can rise 4-6 °C above those of the rural areas (Nichol 2005), which will affect building energy performance as well as external pedestrian comfort and the use of outdoor spaces (Huang et al. 2016). To fully understand a buildings thermal and energy performance one should consider the context of its neighbouring buildings. Hong Kong's high-rise towers, however energy-efficient they may be, can create the 'wall effects'(Wong et al. 2011) which uplift localized air temperature and stagnates airflow (Lau & Ng 2013). To what extend does the urban microclimate in high-density cities affect building energy use remains understudied.

This interdependency of buildings with their microclimate calls for a new approach to the design of buildings within an urban cluster. In practice, most buildings are not designed to operate in the actual surrounding microclimate. Generally, building energy models use meteorological weather data that are obtained from rural weather stations. Models such as EnergyPlus (Crawley et al. 2001), Ecotect (Yang et al. 2014), or IES VE (Crawley et al. 2008) do not normally account for localized microclimate; Instead, designers rely on weather data measured at remote rural stations which differ considerably from those of an urban site. Some take into account the urban climate effect at city-scale through generalised modifications to standard weather data to uplift temperatures (Bueno et al. 2013). However, they do not account for the combined modifying effect of solar radiation, air temperature and wind flow. This gap in energy modelling is critical at the scale of building clusters and the space in-between (50-500m), which applies to most city planning and development projects. Urban climatology models have been developed at a larger at city-scale (>1km) (Arnfield 2003), but this is not particularly useful for the design of individual buildings in their immediate urban context. Despite the apparent needs in design practice, rarely are there tools that can readily assess the interactions between urban microclimate and building energy performances (Bouyer et al. 2011). The Computational Fluid Dynamics (CFD) method is the primary tool applied in urban microclimate analysis (Chen & Srebric 2000) (Bruse & Fleer 1998). However, it is computationally expensive and cannot be easily coupled with other simulation platforms (Novoselac & Srebric 2002), and therefore unsuitable to assess large districts and complex urban configurations (Yang & Li 2009). Recent urban energy assessment tools such as CitySim (Robinson et al. 2009) and UMI (Christoph F et al. 2013) have made significant progress in the European and North American context; yet both accept simplified assumptions in airflow or air temperature which may limit their application for high-density cities.

The building energy model HTB2 has been developed to simulate large numbers of buildings simultaneously using Sketch-up (Trimble Inc. 2016) to quickly set up the various input files that describe the buildings, layout, construction, HVAC systems, occupancy and weather data, with plugins for calculating solar shading from neighbouring buildings, topography and landscape features(Jones, Phil; Lannon, Simon; Li, Xiaojun; Bassett, Thomas; Waldron 2013). However, this does not account for microclimate related external temperatures and wind flow. The Urban Microclimate Model (UMM) (Huang et al. 2015) uses a multizone airflow network model to assess canopy layer airflow in high-density cities, where air mass flow within an interconnected network of external zones is driven by pressure and density differences.

This paper presents the development an integrated model, which couples a multizone urban microclimate airflow network model (UMM) with the building energy model (HTB2). The models exchange air and surface temperature data on an hourly basis. The model also includes the consideration of anthropogenic heat gains from traffic and waste heat from building HVAC systems. Results have been evaluated using a field experiment conducted in the Sai Ying Pun Neighbourhood in Hong Kong.

Simulation Methods

The integrated model is based on the Urban Microclimate Model (UMM) (Huang et al. 2015) and a Building Energy Model (BEM) of HTB2 (Jones, Phil; Lannon, Simon; Li, Xiaojun; Bassett, Thomas; Waldron 2013). The UMM provides localized external zone air temperatures to HTB2, while external building surface temperature and HVAC exhaust data, calculated by HTB2, are returned to the UMM on an hourly time step. There are separate plug-ins for green landscape features and transport related anthropogenic heat gains from transport.

Building Energy Model – HTB2

The software employed in the research included HTB2 and VirVil SketchUp (Jones et.al, 2013), both were developed at the Welsh School of Architecture, Cardiff University. HTB2 is typical of the more advanced numerical models developed over thirty years and extensively tested and validated by the IEA Annex 1 (Oscar Faber and Partners, 1980), IEA task 12 (Lomas, 1994) and the IEA BESTEST (J. Neymark et al, 2011). HTB2 uses input data, hourly climate for the location, building materials and construction, spatial attributes, system and occupancy profiles to calculate the energy required to maintain specified internal thermal conditions (P.T. Lewis, D.K. Alexander, 1990). Due to its advantages of flexibility and ease of modification, HTB2 is well suited for use in the field of energy efficiency and sustainable design of buildings. VirVil SketchUp is an extension development of HTB2 for urban scale modelling. By linking SketchUp with HTB2, it can carry out dynamic thermal simulation for multiple buildings in a community or urban scale, with consideration to the overshadowing impacts from the neighbourhood.
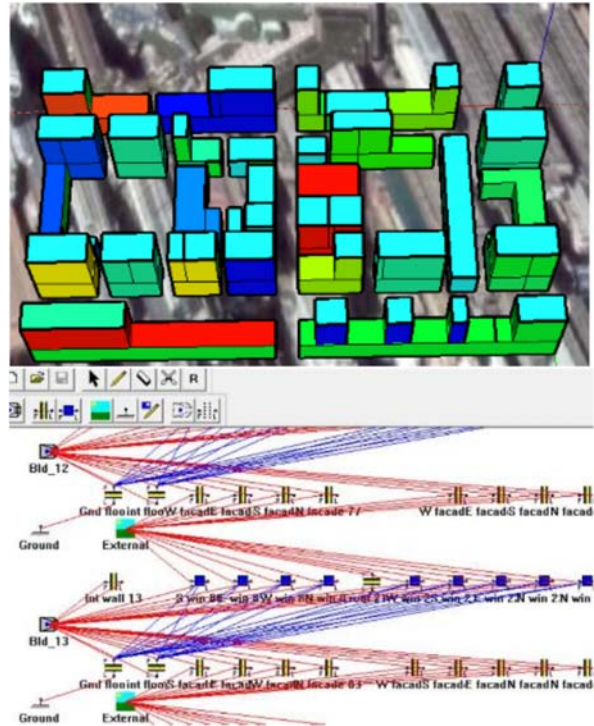

Fig. 1 A Sketchup model of a development, which is transformed by the Virvil plugin to a network (schematic) form, required by the HTB2 Building Energy Model (HTB2 User manual 2.10)

A MultiZone Model for Urban Microclimate

The Urban Microclimate Model (UMM) is a multizone airflow network model (Huang et al. 2015) that can be used to assess the mass and energy of the air in urban environments. It uses a simplified approach that was first developed to describe indoor environments (Musy et al. 2001) and later applied for outdoor spaces (Rao et al. 2011). The urban canopy layer (UCL) is divided into a series of semi-enclosed 'zones' resembling roofless buildings. The air within the UCL exchanges mass and energy with the zone's surrounding urban surfaces, anthropogenic heating/cooling sources, the Urban Boundary Layer (UBL) above, and the Rural Boundary layer (RBL) on its side (Fig. 2). To simplify the process, it is assumed that the airflow is driven by pressure, temperature and density differences, upholding the conservation of mass and energy, while relaxing the momentum conservation equations. It is assumed that that this relaxation method is appropriate for high-density cities where wind-driven flow are often stagnant, at which time buoyancy flow dominates (Yang & Li 2009).
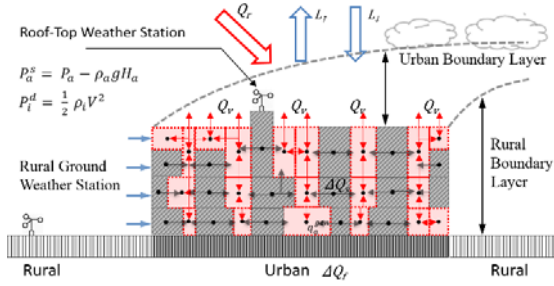
Fig. 2 Schematic depiction of the urban microclimate model

The air within each zone is characterized by a uniform temperature (T_i) and density (ρ_i). The zonal air pressure (P_i^e) at any given height (He) is expressed as $P_i^e = P_i^c - \rho_i g H_e$ (1), where P_i^c is the air pressure at the geometric centre of the zone, and H_e is the vertical distance from the zone centre. Pressure, temperature, and density observe the law of the ideal gas $\rho_i = P_i / R_{air} T_i$ (2) (R_{air} is the gas constant). The airflow rate F_{ij} from zone i to neighbouring zone j is a function of pressure and density differences at the border and characteristics of the openings $F_{ij} = f[\Delta P_{ij}, \Delta \rho_{ij}, A_{ij}]$ (3). Mass conservation is observed in each zone $V_i \frac{\partial \rho_i}{\partial t} + \sum_{j=1}^{J} F_{i,j} = 0$ (4). Since mass changes caused by density difference is often negligible, we have $\sum_{j=1}^{J} F_{i,j} = 0$ (5). Airflow models calculating the F_{ij} and F_{ji} are provided in the authors' earlier work (Huang et al. 2015).

The energy conservation equation for the body of air within zone i is expressed in formula (6), which describes heat transfer from solid surfaces, airflows to and from neighbouring zones, thermal massing, and anthropogenic heat generation (vehicles & AC units):

$$\frac{\partial T_i}{\partial t} C_p \rho_i V_i = \sum_{k=1}^{K} hA(T_k^{surf} - T_i) + \sum_{a=1}^{A} \lambda q_a^{gen} + \sum_{j=1}^{J}(C_P F_{ij} T_i - C_p F_{ji} T_i) \quad (6)$$

where K is the number of enclosing solid surfaces, each with the surface temperature of T_k^{surf}; h is the convective heat transfer coefficient between solid surfaces and air; T_k^{surf} is the temperature for each solid surface; A is the number of active heat sources within zone i, q_a^{gen} and λ are the power and operational coefficient of each heat source; F_{ij} and F_{ji} are the airflow rates between zone i and neighbouring zone j; j is the number of neighbouring zones; C_P and V_i are the specific heat capacity and volume of the zonal air.

Combination of UMM & BEM
UMM and HTB2 are coupled on an hourly time-step. At the completion of a time-step, HTB2 passed updated values of the building surface temperatures to UMM.It also sends data on any ventilation exhaust that is input to the outdoor zones. At this point HTB2 pauses. UMM then computes a new set of outdoor zone temperatures,

which it passes to HTB2. Then HTB2 proceeds with the next hourly time step. At each hour both models are updated with local weather station weather data, and UMM is updated with hourly data for plant cooling and traffic heat gains. Fig. 3 below summarises this process.
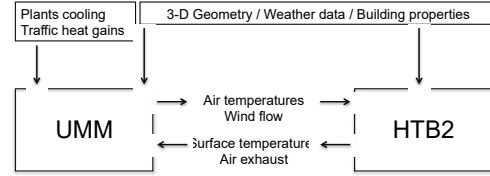

Fig. 3. Conceptual strategy for the integrated urban microclimate and building energy model.

The main modification to HTB2 is the reference to outdoor air temperature. Instead of each external wall, window, roof element and the indoor zone using a single external air temperature taken from the weather file, it uses the individual outdoor zones set up by UMM. These zones will have increased or decreased values in comparison to the weather data file, depending on Urban Heat Island effects. The modification of UMM, is that it takes HTB2 building external surface temperatures, rather than calculating them internally. The ground surface temperature was calculated as wall elements in HTB2, similar to calculating internal ground floors, although they have direct solar gains and shading applied to their external surface, as any other external wall or roof element.

The system reaches an equilibrium if airflow, pressure, and temperature stabilize. Thus, the solver for the integrated model applies a three-loop structure: in Loop A, the zonal pressure P_i and inter-zone airflow F_{ij} were calculated by iteratively solving the pressure balance and airflow equations (equation (3) to (5)), convergence was reach if Pressure Residual, defined as the maximum differences of P_i between iterations, drop below the threshold level. In Loop B, the air temperature of each zone T_i was solved iteratively using equation (8) using P_i and F_{ij} derived from Loop A. T_i was input in Loop A again to calculate the new inter-zonal airflow $\acute{F}_{ij}$. The results reach convergence only if the maximum difference between $\acute{F}_{ij}$ and F_{ij}, known as the Flow Residual computed in the Overall Loop, decrease within a predefined threshold.

Field Studies
To evaluate the predicted localized external zone air temperature and building façade surface temperature, a field experiment was carried out in a cluster of 28 buildings in Sai Ying Pun, a high-density neighbourhood in Hong Kong. Measurements were collected on the 9th December 2014, a sunny winter day. This day was used to avoid uncertainties associated with anthropogenic heat emission from window AC units. The measurements were carried out from 08:00 to 22:00 on the study day.

Fig. 4 shows the overall site and the location of four measurement points (A,B,C and D). Site A is on the sidewalk of Des Voeux Street, a main busy street with 4-lane vehicular traffic. Site B is at the road intersection between the Western Rd. and Queen's Rd. West; Site C is in Sai Yuen Lane, a narrow alleyway inside the residential block. Site D is at the end of Chung Ching Street. The street width, density and configurations vary among the 4 sites, providing a potential variation in microclimate conditions.

Fig. 4 The Sai Ying Pun area and 4 measurement locations (A, B, C, & D) Source: Google Earth (300 by 160 meters)

Air temperature and wind speed were measured at the four locations at 1.5 meters above ground. An infrared camera (FLIR E40-NIST) was used to measure the surrounding surface temperatures at hourly intervals. Vehicular and pedestrian traffic were recorded at Site A and Site B to calculate the anthropogenic heat gains. A 3-min video was recorded at hourly interval, from which the number of pedestrians and automobiles were counted as well as the fleet composition.

The weather data were obtained from the Hong Kong Observatory weather station located in Hong Kong Park and the Green Island, the nearest two locations from the study site. Table 1 summeried hourly weather conditions on 9th December, 2014 from 8:00-22:00. The air temperature and pressure data were taken from the Hong Kong Park (32 meter above sea level), while the wind speed and direction were measured on the Green Island (reference heigh 107 meter above sea level) which was later adjusted to the reference height of 10m above the ground. The input wind speed for the simulation domain was adjusted from the measurement height following the power law distribution.
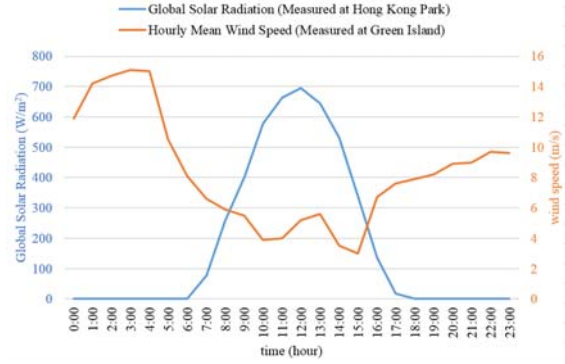

Fig. 5 Meteorological conditions (solar radiation and wind speed) during the 24-hour cycle on Dec.9, 2014.

Table 1 Input houly weather data measured from nearby Hong Kong observatory weather station network on 9th December, 2014.

Hour	Atmospheric Pressure (kPa)	Air Temp. (°C)	Wind speed* (m/s)	Wind direction (° from north)
8:00	102.31	18.4	2.3	30
9:00	102.39	19.1	2.1	30
10:00	102.35	20	1.5	50
11:00	102.29	20.6	1.5	60
12:00	102.20	20.8	2.0	50
13:00	102.09	20.9	2.2	50
14:00	101.99	20.5	1.4	50
15:00	101.93	20.3	1.2	190
16:00	101.94	19.7	2.6	50
17:00	101.97	19.7	2.9	50
18:00	102.02	19.5	3.1	50
19:00	102.05	19.8	3.2	60
20:00	102.10	19.8	3.4	60
21:00	102.14	19.7	3.5	50
22:00	102.14	19.6	3.8	50

* wind speed was adjusted to the reference height of 10m above ground.

Traffic waste heat intensity q_i^{gen} for zone i is estimated from vehicle counts conducted on-site, fleet composition, and mean vehicle speed. q_v^{gen} is expressed in the formula (7) below

$$q_i^{gen} = \sum_{m=1}^{M} \frac{N_m}{V} L_i Q_m \qquad (7)$$

N_m is the vehicle count for vehicle type m (per hour); the data were provided in Table 2 and Table 3 for the two major roads, Des Voeux Road West and Western Street respectively. M is the model of vehicles observed in this study (Car, Mini Bus, Light Truck, Bus). V is the mean vehicle speed; L_i is the length of vehicular road embedded in each zone. $Q_m$is the power intensity for each type of vehicles which can be calculated using mean Fuel Consumption Per Distance Travelled (Table 4) and standard heat content for fuel (7594.0 Kcal/l for gasoline).

Table 2 Hourly vehicle count by type on Des Voeux Road West during the study day

Time	Car	Mini Bus	Truck	Bus
09:00-10:00	1248	272	464	352
10:00-11:00	1376	224	560	304
11:00-12:00	1328	240	624	288
12:00-13:00	1136	224	416	320
13:00-14:00	1504	192	336	256
14:00-15:00	1024	208	256	176
15:00-16:00	1168	240	256	320
16:00-17:00	1504	160	192	240
17:00-18:00	1408	208	176	256
18:00-19:00	976	320	144	384
19:00-20:00	960	304	32	352
20:00-21:00	960	128	48	320
21:00-22:00	784	48	32	256

Table 3 Hourly vehicle count by type on Western Street during the study day

Time	Car	Mini Bus	Truck	Bus
09:00-10:00	1200	240	304	144
10:00-11:00	1440	272	448	192
11:00-12:00	1104	320	480	160
12:00-13:00	1168	208	512	224
13:00-14:00	1296	288	384	176
14:00-15:00	1248	272	288	144
15:00-16:00	976	192	192	240
16:00-17:00	1040	224	240	272
17:00-18:00	1328	160	144	192
18:00-19:00	1152	256	192	304
19:00-20:00	864	192	80	240
20:00-21:00	656	80	32	112
21:00-22:00	368	48	32	80

Table 4 Vehicle types and fuel consumption data used in this study

Vehicle Types	Fuel Consumption Per Distance Travelled (Liter /100 km)
Car (Sedan/Van/SUV)	14.0
Mini Bus	17.7
Light Truck	20.0
Bus (Double-Decker)	66.2 (Diesel)

Results & Discussion

The integrated UMM HTB2 model was applied to simulate the Sai Ying Pun neighbourhood. The model domain consisted of 71 external zones and 28 buildings. The external zones were divided into two vertical layers, allowing conditions to vary at near-ground (0-20m) and higher above (20-50m). The model domain and four measurement locations in the field studies are shown in Fig. 6.
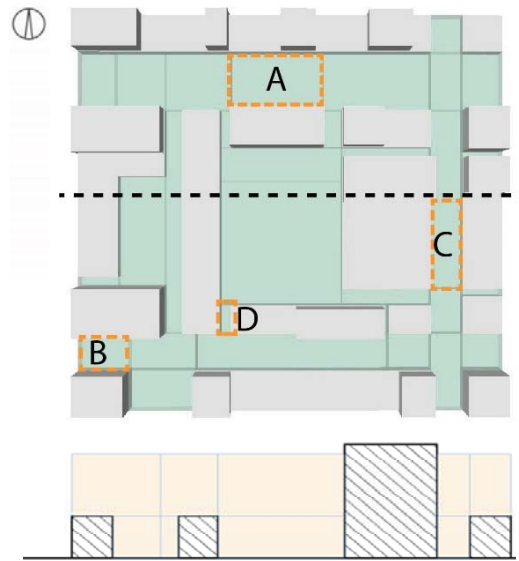

Fig. 6 Model domain, 3D building geometries and measurement locations (shown in both plan and section)
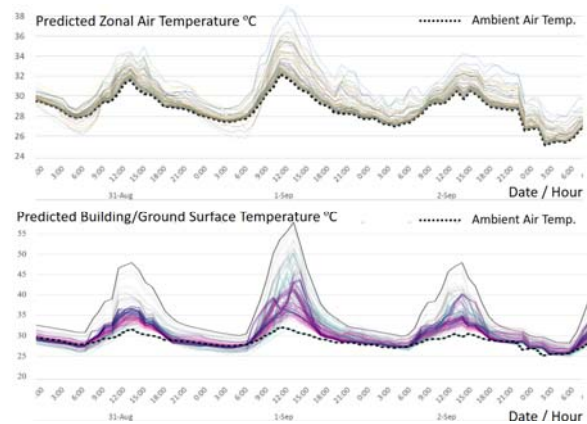

Fig. 7 Predicted zonal air temperature and surface temperature using the integrated model.

Model results included surface temperature, air temperature and wind speed at 4 locations. Fig. 8 shows predicted air temperature at 4 locations in comparison with measurement results. Due to the dual influence from solar radiation and anthropogenic heat exhaust, air temperatures in street canyons can be up to 3 ℃ higher than the ambient air temperature measured from the Hong Kong Park. The "heat island effect" of the street canyon appears more significant when the external wind speed is low.
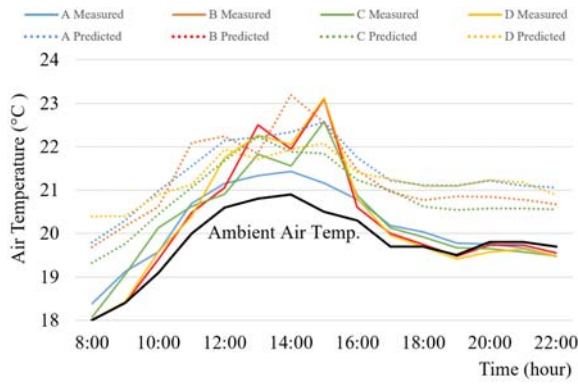
Fig. 8 Predicted and measured air temperature at four measurement points using the integrated model. The black dash line is the ambient air temperature measured from the Hong Kong Park Weather Station.
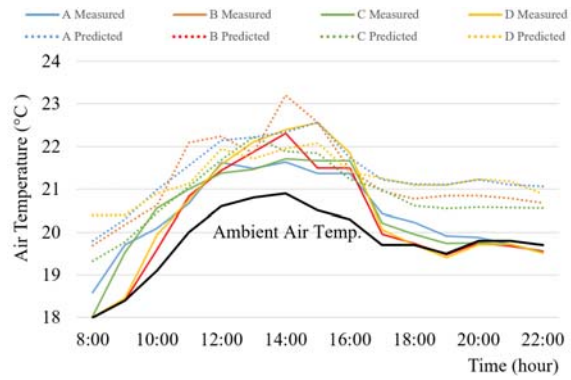
Fig. 9 shows the air temperature distribution and airflow direction at 10:00 am. Results showed that narrow street canyons, measured in terms of height-to-width ratio, featured lower air temperature compared with those of a wider one.
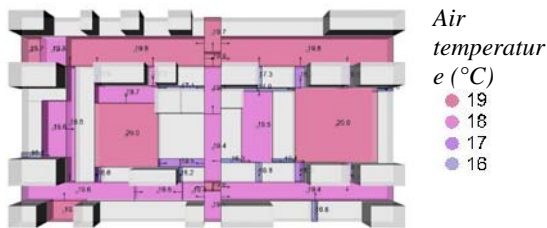

Air temperature (°C)
- 19
- 18
- 17
- 16

Fig. 9. Predicted air temperature (in color) and airflow direction (in arrow) at 10 am Dec 9, 2014

Impact of Traffic Waste Heat

A sensitivity analysis of traffic waste heat shows that localized air temperature of street-canyon can rise up to 1.3 ℃ due to the presence of traffic. The phenomenon of traffic-related warming appears more significant when external wind is weak. Fig. 10 shows predicted air temperature at four locations without data inputs from traffic waste heat. Measured air temperature at point B is 1.3 ℃ lower than the equivalent shown in Fig. 8 at 15:00, the hour with the lowest external wind speed.

Fig. 10 Predicted and measured air temperature at four measurement points without traffic waste heat input. The black dash line is the ambient air temperature measured from the Hong Kong Park Weather Station.

Computing Efficiency

An advantage of the integrated model lies in its computing speed. On average, it takes 1-2 mins for results of each hour for the study site. This is a significant improvement over previous attempts using coupled CFD and building energy models. Residuals for loop A (pressure), B (temperature), and Overall (flow) are charted in Fig. 11 for a single hour at 8:00 Dec.9, 2014.
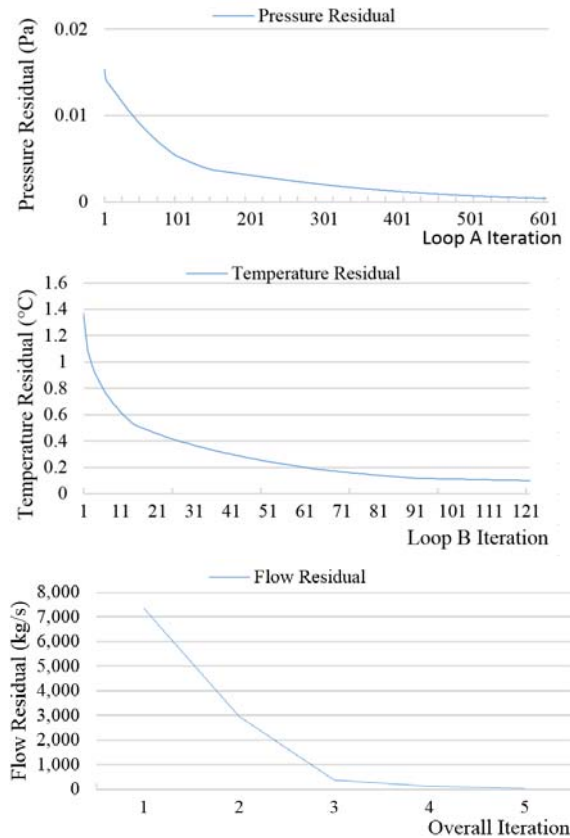

Fig. 11 Model convergence at 8:00 Dec.9, 2014. Loop A, Loop B, and Overall Loop reached satisfactory convergence with Pressure Residual, Temperature

Residual, and Flow Residual decreasing below their threshold levels respectively.

Conclusions

An integrated model for urban microclimate and building energy was developed. Field measurements were conducted in Hong Kong's high-density urban area to partially evaluate the model performance. Simulation results of the outdoor air and building façade temperatures within street canyons showed considerable variations among measurement spots.

Major contributions of this research lies the following aspects. First, we developed and evaluated an integrated model that can describe the energy performance of a cluster of buildings in place of the surrounding microclimate; the research contributed to the literature of environmental modelling at the scale of a cluster of buildings (50-500m) in which most buildings and urban design projects are commissioned.

Second, localized urban microclimate can raise street canyon temperature up to 2.5 ºC above those of the ambient air. Traffic waste heat can raise street-canyon air temperature by 1.3 C when wind-driven ventilation is weak.

Third, the integrated model can be a useful tool to support sustainable design at early stage. The advantage of the new model lies in its computing efficiency. This allows coupled simulation of urban microclimate and building energy to be executed on weekly and seasonal basis.

A major limit for the current study is that the impact of urban microclimate on building energy use cannot be fully identified using existing data of the winter season. Currently, the research team was only able to complete field measurement in winter on Dec.9, 2014, in which neither cooling nor heating energy are significant under Hong Kong's mild weather -- the air temperature was between 18.9 to 21.0 ºC. A sensitivity study on the impact of building waste heat, together with more field studies, are scheduled for the next step.

The next step is to further improve solver efficiency and Given the uncertainties associated with a real urban site, anthropogenic heat sources from residential AC units, restaurants, or other sources cannot be accurately measured on-site; this may explain the relatively weak prediction power of the integrated model of on-site air temperature. We plan to further evaluate the integrated model using experiment to be conducted on mock-up sites and scale-models.
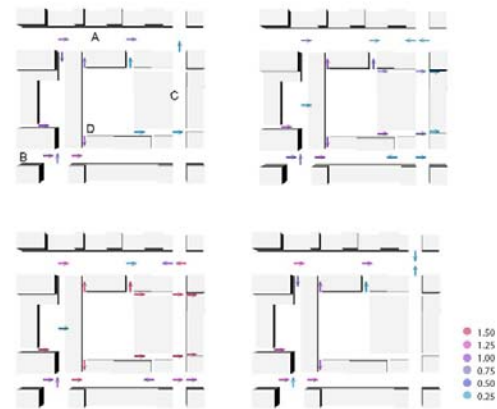
Appendix

Fig. 12, Predicted airflow pattern in Sai Ying Pun neighborhood from the integrated model at 8am, 11am, 3pm and 8pm on Dec.9, 2014.
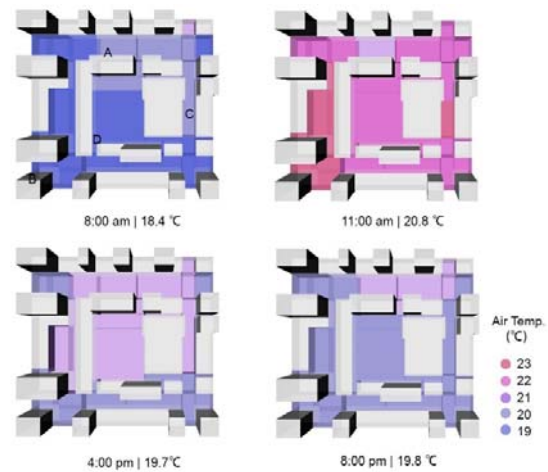

Fig. 13 Predicted zonal air temperature at ground floor in Sai Ying Pun neighborhood from the integrated model at 8am, 11am, 3pm and 8pm on Dec.9, 2014.

Acknowledgement

References

Arnfield, J., 2003. Two decades of urban climate research: a review of turbulence, exchanges of energy and water, and the urban heat island. *International Journal of Climatology*, 23(1), pp.1–26. Available at: http://doi.wiley.com/10.1002/joc.859 [Accessed July 14, 2014].

Bouyer, J., Inard, C. & Musy, M., 2011. Microclimatic

coupling as a solution to improve building energy simulation in an urban context. *Energy and Buildings*, 43(7), pp.1549–1559. Available at: http://www.sciencedirect.com/science/article/pii/S0378778811000545 [Accessed August 7, 2015].

Bruse, M. & Fleer, H., 1998. Simulating surface–plant–air interactions inside urban environments with a three dimensional numerical model. *Environmental Modelling & Software*, 13(3–4), pp.373–384. Available at: http://www.sciencedirect.com/science/article/pii/S1364815298000425 [Accessed June 4, 2015].

Bueno, B. et al., 2013. The urban weather generator. *Journal of Building Performance Simulation*, 6(4), pp.269–281. Available at: http://www.tandfonline.com/doi/abs/10.1080/19401493.2012.718797#.V5WGsTSe8g8.mendeley [Accessed June 2, 2016].

Chen, Q. & Srebric, J., 2000. Application of CFD Tools for Indoor and Outdoor Environment Design. *International Journal on Architectural Science*, 1(1), pp.14–29.

Christoph F, R. et al., 2013. Umi - an Urban Simulation Environment for Building Energy Use , Daylighting and Walkability. *Proceedings of BS2013: 13th Conference of International Building Performance Simulation Association*, pp.476–483.

Crawley, D.B. et al., 2008. Contrasting the capabilities of building energy performance simulation programs. *Building and Environment*, 43(4), pp.661–673. Available at: http://www.sciencedirect.com/science/article/pii/S0360132306003234 [Accessed July 9, 2014].

Crawley, D.B. et al., 2001. EnergyPlus: creating a new-generation building energy simulation program. *Energy and Buildings*, 33(4), pp.319–331. Available at: http://www.sciencedirect.com/science/article/pii/S0378778800001146 [Accessed March 24, 2015].

Huang, J. et al., 2016. Outdoor Thermal Environments and Activities in Open Space: An Experiment Study in Humid Subtropical Climates. *Building and Environment*. Available at: http://www.sciencedirect.com/science/article/pii/S0360132316301123 [Accessed April 12, 2016].

Huang, J., Zhang, A. & Peng, R., 2015. Evaluation the MultiZone Modle for Street Canyon Airflow in High-Density Cities. In *14th International Conference of the International Building Performance Simulation Association*. Hyderabad, India. Available at: http://www.ibpsa.org/proceedings/BS2015/p2978.pdf.

Jones, Phil; Lannon, Simon; Li, Xiaojun; Bassett, Thomas; Waldron, D., 2013. Intensive Building Energy Simulation At Early Design Stage. In *Proceedings of BS 2013: 13th Conference of the International Building Performance Simulation Association*.

Lau, K.L. & Ng, E., 2013. An investigation of urbanization effect on urban and rural Hong Kong using a 40-year extended temperature record. *Landscape and Urban Planning*, 114, pp.42–52. Available at: http://linkinghub.elsevier.com/retrieve/pii/S0169204613000443 [Accessed October 5, 2014].

Musy, M. et al., 2001. Generation of a zonal model to simulate natural convection in a room with a radiative/convective heater. *Building and Environment*, 36(5), pp.589–596.

Nichol, J., 2005. Remote sensing of urban heat islands by day and night. *Photogrammetric Engineering and Remote Sensing*, 71(May), pp.613–621. Available at: http://www.scopus.com/inward/record.url?eid=2-s2.0-31344433406&partnerID=40&md5=d428b47f298d81de9d9917f80c47454b.

Novoselac, A. & Srebric, J., 2002. A critical review on the performance and design of combined cooled ceiling and displacement ventilation systems. *Energy and Buildings*, 34(5), pp.497–509. Available at: http://www.sciencedirect.com/science/article/pii/S0378778801001347 [Accessed October 20, 2015].

Rao, R., Luo, Q. & Li, B., 2011. A simplified mathematical model for urban microclimate simulation. *Building and Environment*, 46(1), pp.253–265. Available at: http://www.sciencedirect.com/science/article/pii/S0360132310002246 [Accessed September 23, 2015].

Robinson, D. et al., 2009. CITYSIM: Comprehensive Micro-Simulation Of Resource Flows For Sustainable Urban Planning. In *International IBPSA Conference*. Glasgow: IBPSA, pp. 1083–1090.

Trimble Inc., 2016. SketchUp. Available at: http://www.sketchup.com/.

Wong, M.S., Nichol, J. & Ng, E., 2011. A study of the "wall effect" caused by proliferation of high-rise buildings using GIS techniques. *Landscape and Urban Planning*, 102(4), pp.245–253. Available at: http://www.sciencedirect.com/science/article/pii/S0169204611001964 [Accessed October 7, 2015].

Yang, L., He, B.-J. & Ye, M., 2014. Application research of ECOTECT in residential estate planning. *Energy and Buildings*, 72, pp.195–202. Available at: http://www.sciencedirect.com/science/article/pii/S0378778813008578 [Accessed June 8, 2015].

Yang, L. & Li, Y., 2009. City ventilation of Hong Kong at no-wind conditions. *Atmospheric Environment*, 43(19), pp.3111–3121. Available at: http://www.sciencedirect.com/science/article/pii/S1352231009002015 [Accessed October 8, 2015].